Talanta 107 (2013) 277–283

Contents lists available at SciVerse ScienceDirect

Talanta

journal homepage: www.elsevier.com/locate/talanta

Detection of Ag^+ ions and cysteine based on chelation actions between Ag^+ ions and guanine bases

Xia Chen [a,b], Yinran Chen [a,b], Xiaodong Zhou [a,b,*], Jiming Hu [a,b,*]

[a] Key Laboratory of Analytical Chemistry for Biology and Medicine (Ministry of Education), College of Chemistry and Molecular Sciences, Wuhan University, Wuhan, Hubei 430072, China

[b] Institute of Analytical Biomedicine, College of Chemistry and Molecular Sciences, Wuhan University, Wuhan, Hubei 430072, China

ARTICLE INFO

Article history:
Received 4 October 2012
Received in revised form
8 January 2013
Accepted 14 January 2013
Available online 21 January 2013

Keywords:
Fluorescence
Biosensor
Ag^+ ions
Cysteine
Graphene oxide

ABSTRACT

A selective and sensitive fluorescence biosensor for Ag^+ ions and cysteine (Cys) was developed based on the chelation actions between Ag^+ ions and guanine bases of G-rich fluorogenic oligonucleotide (FAM-ssDNA) and the different electrostatic affinity between FAM-ssDNA and graphene oxide (GO). FAM-ssDNA adsorbed onto the surface of GO through π–π stacking interaction between the ring structure in the nucleobases and the hexagonal cells of GO, and the fluorescence of the dye was quenched. In the presence of Ag^+ ions, the random coil structure changed into a G-Ag^+ architecture. As a result, the binding released FAM-ssDNA signal probe from the surface of GO, which disrupted the energy transfer from FAM-ssDNA to GO, recovering the fluorescence emission of FAM-ssDNA. On the other hand, because Cys was a strong Ag^+ ions binder, it could deactivate the sensor fluorescence by rewrapping FAM-ssDNA around GO. In this way, these changes in fluorescence intensity allowed the selective detection of Ag^+ ions and Cys.

1. Introduction

Silver, as a rare but naturally occurring metal, has been widely employed in industries such as electronics and photography. However, Ag^+ ions are assigned to be one of the most toxic forms in aquatic environments, largely because the severe environmental effects and serious medical effects on human health. Also, cysteine (Cys) plays a crucial role in human body. A number of diseases can result from the abnormal of the level of Cys. Cys deficiency will be involved in many syndromes, such as edema, lethargy, hair depigmentation, liver damage, slowed growth and skin lesion [1]. Additionally, the increased cysteine level can lead to a higher risk for cancer and Alzheimer's diseases [2]. So developing a sensitive and selective sensor for detection of Ag^+ ions and Cys is an important issue. Over the past few decades, a number of analysis methods have been developed, including electrothermal atomic absorption spectrometry (ETAAS) [3,4], voltammetry [5–7], inductively coupled plasma atomic emission spectrometry (ICP-AES) [8], inductively coupled plasma mass spectroscopy (ICP-MS) [9] and potentiometry [10,11]. Though these methods have high selectivity and sensitivity, they are somewhat complex, costly, and time consuming. Recently, some researches showed that metal ions including Ag^+ ions could selectively bind to a few native bases in DNA, in this way "metal-base pairs" [12,13] were created. Due to the special selectivity and potential in sensing applications, a number of Ag^+ ions and Cys sensors [14,15] had been constructed, based on the formation of strong and stable C–Ag^+–C complexes. Shen's group [16,17] reported that Ag^+ ions could disrupt G-quadruplex structures by interacting with guanine bases. Both G-quadruplex-hemin DNAzyme-based colorimetric method and proposed fluorescence-based method were created. As a strong binder of Ag^+ ions, Cys could interact with Ag^+ ions and neutralized its activity, resulting in the reformation of G-quadruplex structures and quantitation of Cys.

Herein, we present a rapid assay for highly sensitive and selective detection of Ag^+ ions and Cys, based on chelation actions between Ag^+ ions and G-rich FAM-ssDNA. In order to increase the signal-to-noise ratio of FAM-ssDNA probes, highly efficient nanoquenchers, such as AuNPs [18–21] and SWNTs [22–25], were more attractive than the traditional organic quenchers, based on their rich chemical, optical and mechanical properties. For example, carbon nanotubes [26–29] and single-stranded DNA (ssDNA) assemblies had been used for homogeneous detection of biomolecules. Recently, graphene oxide (GO) [30,31] was predicted through theoretical calculations to be a super quencher with a long-range resonance energy transfer property. The sensing mechanism was as follows (Fig. 1), in the

* Corresponding authors at: College of Chemistry and Molecular Sciences, Key Laboratory of Analytical Chemistry for Biology and Medicine (Ministry of Education), Wuhan University, Wuhan, Hubei 430072, China. Tel.: +86 27 68752439 8116; fax: +86 27 68752136.
E-mail addresses: zhouxd@whu.edu.cn (X. Zhou), jmhu@whu.edu.cn (J. Hu).

0039-9140/$ - see front matter © 2013 Elsevier B.V. All rights reserved.
http://dx.doi.org/10.1016/j.talanta.2013.01.025

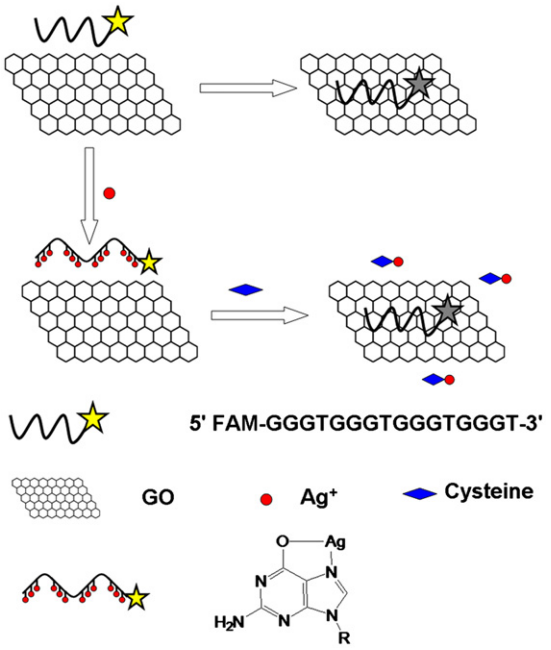

Fig. 1. Schematic representations of Ag^+ ions and Cys detection mechanism using the FAM-ssDNA/GO system based on a fluorescence spectroscopy method.

absence of Ag^+ ions, FAM-ssDNA could interact noncovalently with GO, and formed stable complexes with GO by means of π–π stacking between nucleotide bases and GO, which completely quenched the fluorescence of FAM-ssDNA. However, in the presence of Ag^+ ions, the N_7 and C_6O groups in guanine bases of G-rich FAM-ssDNA were chelated, disrupting the formation of ssDNA/GO complexes. FAM-ssDNA was far away from the surface of GO and the fluorescence was recovered. We hypothesized that the increase of fluorescence intensity was dependent on the concentration of Ag^+ ions, a new "turn on" Ag^+ ions detection method might be developed. Considering that Cys was a strong binder of Ag^+ ions, the structure of G-Ag^+ was destroyed, resulting in the re-formation of ssDNA/GO complexes and the decrease of fluorescence. The amount of Cys could be easily measured according to the decrease of fluorescence. Therefore, this method was further exploited as a facile, cheap, sensitive and selective "turn-off" sensor for Cys.

2. Experimental section

2.1. Chemicals and apparatus

The oligonucleotides (FAM-ssDNA: 5′-FAM-GGGTGGGTGGGT GGGT-3′, FAM-TBA: 5′-FAM-TGGTTGGTGTGGTTGG-3′) were synthesized by Shanghai Sangon Biotechnology Co. Ltd. (Shanghai, China). Graphene oxide (GO) was purchased from Sinocarbon Materials Technology Co., Ltd. The used metal salts, $AgNO_3$, $Mg(NO_3)_2$, $Cu(NO_3)_2$, $Cr(NO_3)_3$, $Ni(NO_3)_2$, $Co(NO_3)_2$, $Al(NO_3)_3$, $Fe(NO_3)_3$, $MnAc_2$, $ZnCl_2$, $CaCl_2$, LiCl, $Hg(NO_3)_2$, $Cd(NO_3)_2$ and CuCl were of analytical grade and used as received without further purification. The amino acids used in this work included Cys, Ala, Arg, Asn, Asp, Glu, Gly, His, Ile, Leu, Lys, Met, Phe, Pro, Ser, Thr, Trp, Tyr, Val, cystine and glutathione. All working solutions were prepared with Tris buffer solution (20 mM, 100 mM $NaNO_3$, pH 8.0). Millipore water with an electrical resistance larger than 18.2 MΩ was used throughout. All the oligonucleotide solutions and buffers in the experiments were prepared using sterile water. Fluorescent emission spectra were performed on a F-4600 fluorescence spectrophotometer, Hitachi High Technology Co., Ltd. (Tokyo, Japan). The excitation wavelength was set at 480 nm, and the emission wavelength was set at 520 nm [32].

2.2. Assay for Ag^+ ions (a) and Cys (b)

Before use, GO powder was dissolved in water and then sonicated for 8 h to give a homogeneous brilliant yellow solution. (a) FAM-ssDNA (0.2 μM) was mixed with different concentrations of Ag^+ ions for 30 min, then GO was added into each mixture to make the final volume 200 μL. The final concentration of GO was 80 μg mL^{-1}. The mixtures were vortexed to mix all the reagents and then incubated for another 30 min. Subsequently, the mixtures were placed in the quartz cuvette to measure the fluorescence intensity. To confirm the selectivity of the method, the other metal ion stock solutions instead of Ag^+ ions were used to react with above system and performed in the same way. (b) FAM-ssDNA (0.2 μM) and Ag^+ ions (10 μM) were mixed first, then different concentrations of Cys were added. After the resulting solutions were incubated for 30 min, GO was added into each mixture to make the final volume 200 μL. The final concentration of GO was 80 μg mL^{-1}. The mixtures were vortexed to mix all the reagents and then incubated for another 30 min. Subsequently, the mixtures were placed in the quartz cuvette to measure the fluorescence intensity. To confirm the selectivity of the method, the other amino acid stock solutions instead of Cys were used to react with above system and performed in the same way. All experiments were performed at room temperature.

2.3. Detection of Ag^+ ions (a) in East lake water and Cys (b) in urine

FAM-ssDNA (0.2 μM) was incubated with East lake water first, and reacted for 30 min after the addition of different concentrations of Ag^+ ions. Subsequently, GO and appropriate aliquot of buffer were introduced to make each reaction solution 200 μL. The mixtures were incubated for 30 min and the fluorescence spectra were monitored at room temperature. (b) FAM-ssDNA (0.2 μM) was mixed with Ag^+ ions (10 μM) first, and reacted for 30 min after the addition of urine and different concentrations of Cys. Subsequently, GO and appropriate aliquot of buffer were introduced to make each reaction solution 200 μL. The mixtures were incubated for 30 min and the fluorescence spectra were monitored at room temperature.

3. Results and discussion

3.1. Design strategy based on graphene oxide sensing platform

As shown in Fig. 2, the feasibility of the strategy was evaluated. Owing to the stacking interactions between nucleotide bases and GO, FAM-ssDNA was absorbed rapidly on the surface of GO. Therefore, the fluorescence of 0.2 μM FAM-ssDNA was quenched at least 90% by 80 μg mL^{-1} GO (curve *a*) due to FRET between FAM and GO, indicating the strong quenching effect of GO on the fluorescence of FAM. The FAM-ssDNA we used was rich in guanine bases, which could capture Ag^+ ions and disrupt the formation of FAM-ssDNA/GO complexes. In the presence of 10 μM Ag^+ ions, the random coil FAM-ssDNA changed its conformation, thus weakening the π–π stacking interactions between DNA nucleotide bases and GO, finally leading to the recovery of fluorescence (curve *b*). However, the binding affinity of Ag^+ ions for Cys was much stronger than that for guanine bases, and therefore Cys would remove Ag^+ ions from FAM-ssDNA by working with its active sulfhydryl group and thus FAM-ssDNA

was set free again. Hence, the addition of 10 μM Cys led to the occurrence of FRET and the fluorescence quenching of FAM-ssDNA again (curve *c*).

The effect of Ag^+ ions on the yield of the dye fluorescence was also investigated. As shown in Fig. 3, the yield of 0.2 μM FAM-ssDNA fluorescence was enhanced over one time by the addition of 10 μM Ag^+ ions, however, such enhancement could not be observed with the addition of Hg^{2+} ions or any other metal ions. This phenomenon [33] was attributed to the fact that the interaction between Ag^+ ions and the dye changed the concentration of the various ionic forms of fluorescein, which was responsible for the change in the yield of the fluorescence emission. These results suggested that Ag^+ ions had a positive effect on the yield of the fluorescence emission of FAM-ssDNA, which greatly improved the sensitivity for the detection of Ag^+ ions.

3.2. Optimization of the variables of the measuring system

The sensing conditions for this part of experiment, including GO concentration, pH value, addition order of each reagent and reaction time for fluorescence quenching and restoration were all investigated and optimized.

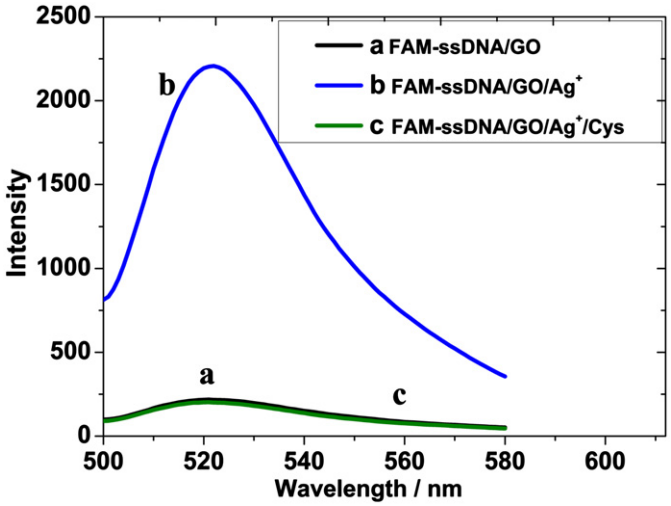

Fig. 2. Fluorescence spectra of FAM-ssDNA at different conditions: (a) FAM-ssDNA+GO; (b) FAM-ssDNA+GO+10 μM Ag^+ ions; (c) FAM-ssDNA+GO+10 μM Ag^+ ions+10 μM Cys. All these fluorescence spectra were carried out in Tris buffer (20 mM, 100 mM $NaNO_3$, pH 8.0) and the concentration of FAM-ssDNA and GO were 0.2 μM and 80 μg mL^{-1}, respectively.

First, it was important to optimize GO concentration as this was crucial for the detection. As could be seen in Fig. 4(A), GO could significantly reduce the fluorescence intensity of FAM-ssDNA either in the absence (red) or in the presence (black) of Ag^+ ions, and the inset was the fluorescence enhancement of FAM-ssDNA by 10 μM Ag^+ ions as a function of GO concentration. From Fig. 4(A), we found that when GO was introduced, the background fluorescence of FAM-ssDNA was gradually reduced, and when GO was 80 μg mL^{-1}, the ratio of F/F_0 (F_0 and F were the fluorescence intensities of FAM-ssDNA in the absence and presence of Ag^+ ions, respectively) reached the highest value. As a result, 80 μg mL^{-1} was used as the optimized GO concentration in the following experiments.

The response of the strategy at different pH values was also studied. Fluorescein, a commonly used biological probe, is such an aromatic and highly conjugated molecule. Cook et al. [34] had studied the effect of pH on fluorescein. They found that fluorescein appeared in different forms with the increase of pH, from the non-fluorescent neutral form to the fluorescent carbonxylic acids form (monoanion and dianion). While among the monoanion and dianion forms, the dianion form was more fluorescent. In even more basic solutions (pH=6.47 and higher), the dianion form was the most prevalent form. As a result, the pH values of the reaction buffer could significantly influence the yield of the fluorescence emission of FAM-ssDNA. As could be seen in Fig. 4(B), the fluorescence intensity increased greatly with the increase of pH. The inset was the fluorescence enhancement of FAM-ssDNA by 10 μM Ag^+ ions as a function of pH. When pH was 8.0, the ratio of F/F_0 (F_0 and F were the fluorescence intensities of FAM-ssDNA in the absence and presence of Ag^+ ions, respectively) reached the highest value. As a result, pH 8.0 was selected in this work.

The effect of the addition order of FAM-ssDNA, Ag^+ ions and GO of this system on the fluorescence was also investigated by monitoring the fluorescence intensity as a function of time. First of all, GO could quench the fluorescence of FAM-ssDNA rapidly, it took less than 4 min to arrive at the equilibrium (Fig. 4(C), curve *a*). What was more, comparing with curve *b* and curve *c*, the value of curve *a* was the lowest one, indicating the feasibility of the design. Then we investigated the effect of the addition order on the fluorescence: (1) FAM-ssDNA was mixed with GO at first and then be challenged with 10 μM Ag^+ ions, with the addition of Ag^+ ions, the pre-quenched fluorescence slowly recovered, suggesting that FAM-ssDNA was liberated from the GO surface during its interaction with Ag^+ ions (Fig. 4(C), curve *b*), however, the fluorescence intensity was much lower than that of curve *c*. (2) FAM-ssDNA was incubated with 10 μM Ag^+ ions at room temperature for 30 min first, and GO was then added to the

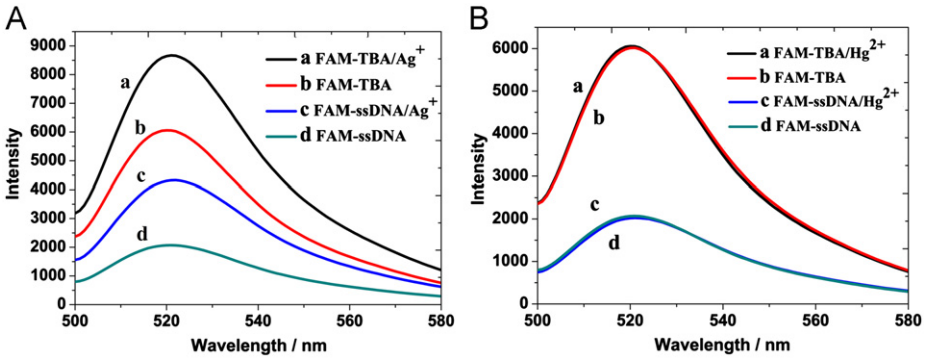

Fig. 3. Fluorescence spectra of (A) 0.2 μM FAM-TBA in the presence (curve *a*) and absence (curve *b*) of 10 μM Ag^+ ions, 0.2 μM FAM-ssDNA in the presence (curve *c*) and absence (curve *d*) of 10 μM Ag^+ ions; (B) 0.2 μM FAM-TBA in the presence (curve *a*) and absence (curve *b*) of 10 μM Hg^{2+} ions, 0.2 μM FAM-ssDNA in the presence (curve *c*) and absence (curve *d*) of 10 μM Hg^{2+} ions. All these fluorescence spectra were carried out in Tris buffer (20 mM, 100 mM $NaNO_3$, pH 8.0).

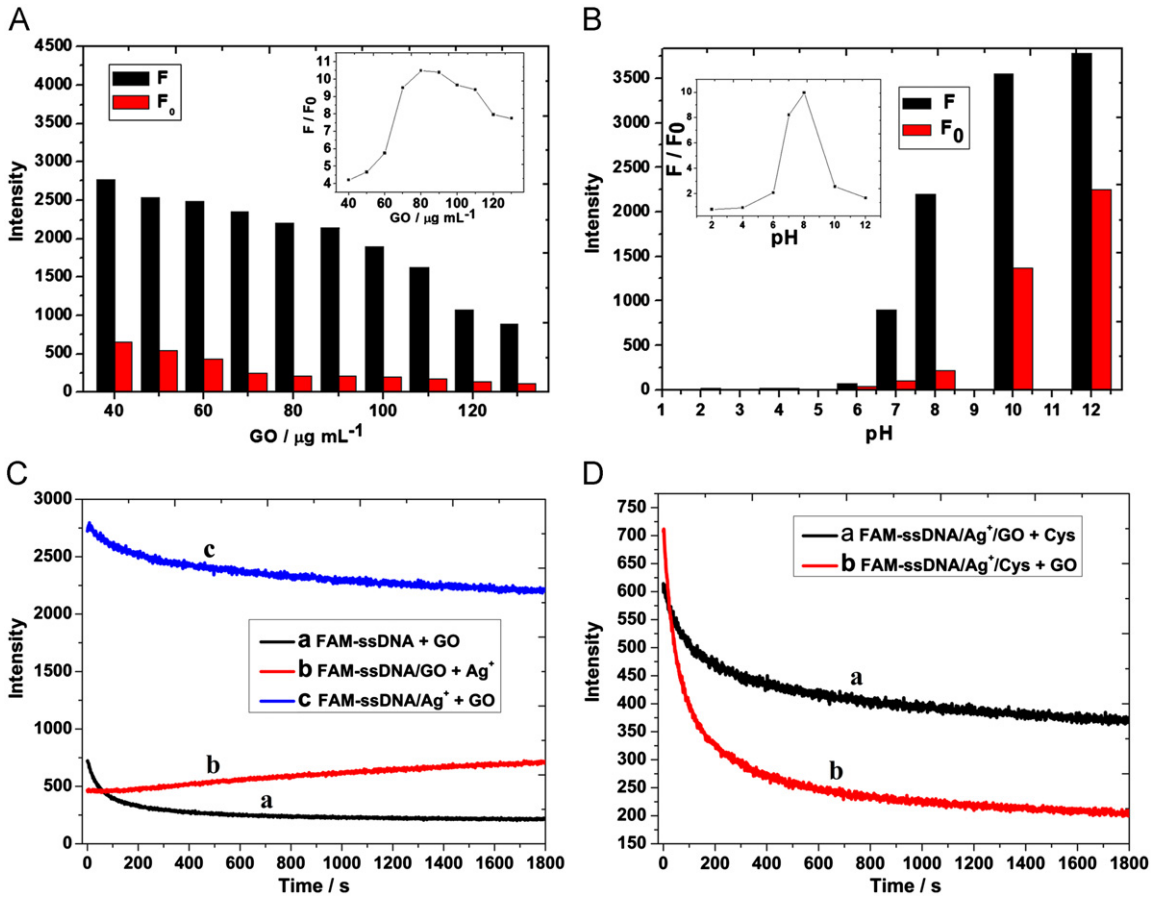

Fig. 4. (A) Effect of GO concentration on the fluorescence intensity of FAM-ssDNA in the absence (F_0) and presence (F) of 10 μM Ag^+ ions. The inset was the fluorescence enhancement of FAM-ssDNA/GO by 10 μM Ag^+ ions as a function of GO concentration. (B) Effect of pH on the fluorescence intensity of FAM-ssDNA in the absence (F_0) and presence (F) of 10 μM Ag^+ ions. The inset was the fluorescence enhancement of FAM-ssDNA/GO by 10 μM Ag^+ ions as a function of pH. (C) and (D) Kinetics study of the fluorescence change for the different addition orders of FAM-ssDNA, GO, 10 μM Ag^+ ions and 10 μM Cys. All these fluorescence spectra were carried out in Tris buffer (20 mM, 100 mM $NaNO_3$, pH 8.0) and the incubation time was 30 min at room temperature with an excitation wavelength of 480 nm (0.2 μM FAM-ssDNA, 80 μg mL^{-1} GO). (For interpretation of the references to color in this figure legend, the reader is referred to the web version of this article.)

mixture before detection. As shown in curve *c* of Fig. 4(C), the fluorescence intensity was decreased at first, while 10 min later the fluorescence intensity no longer gave an obvious change and kept stable. These results implied that G-Ag^+ complexes were formed and the complexes could not interact with GO effectively. Among these two addition strategies, we favored the use of the second addition strategy which was quick in kinetics. Therefore, we chose this addition strategy in the following studies. The addition order for Cys sensing system was the same, as could be concluded from Fig. 4(D), GO was always the last one to add to make sure the complete interactions among FAM-ssDNA, Ag^+ ions and Cys.

3.3. Sensitivity and selectivity toward Ag^+ ions

Free FAM-ssDNA/GO complexes rendered rather weak fluorescence, however, a significant increase in the fluorescence intensity was observed when Ag^+ ions were introduced. Fig. 5(A) showed the fluorescence intensity of FAM-ssDNA/GO complexes upon incubation with a series of concentrations of Ag^+ ions. Along with the increase of the concentration of Ag^+ ions, the resulting fluorescence intensities of FAM-ssDNA/GO complexes were intensified. The addition of Ag^+ ions led to a gradual increase in fluorescence, which reached a steady-state value with addition of 10 μM Ag^+ ions. The resulting calibration curve for Ag^+ ions was shown in the inset of Fig. 5(B), a linear relationship (R^2= 0.9923) was observed with Ag^+ ions from 0.1 to 10 μM and the detection limit for Ag^+ ions was 0.05 μM (based on a signal-to-noise ratio of 3).

We also evaluated the selectivity of this system for Ag^+ ions by testing the response of the assay toward other common metal ions, including Mg^{2+}, Cu^{2+}, Mn^{2+}, Zn^{2+}, Cr^{3+}, Ni^{2+}, Co^{2+}, Li^+, Fe^{3+}, Al^{3+}, Ca^{2+}, Hg^{2+}, Cu^+ and Cd^{2+} (Fig. 5(C)), under the same conditions as those used with Ag^+ ions. Remarkably, no apparent fluorescence changes were observed, only Ag^+ ions resulted in significants fluorescence increases. These results clearly demonstrated that the sensing system was highly selective toward Ag^+ ions over the other metal ions.

In order to evaluate the practical application of this present approach for the analysis of real samples, we challenged this system with East Lake (Wuhan, China) water at room temperature. East Lake water samples were first filtered through a 0.22 μM filter membrane to remove oils, and then be spiked with various concentrations of Ag^+ ions. At last, the fluorescence was recorded through the same strategy as depicted above. As shown in Table 1, the results obtained in real water samples showed good recovery values, which confirmed that the proposed sensor was applicable for Ag^+ ions detection in real samples with other potentially competing species coexisting.

3.4. Sensitivity and selectivity toward Cys

As a sulfur-containing amino acid, Cys plays a crucial role in the human body by allowing the intramolecular cross-linking of

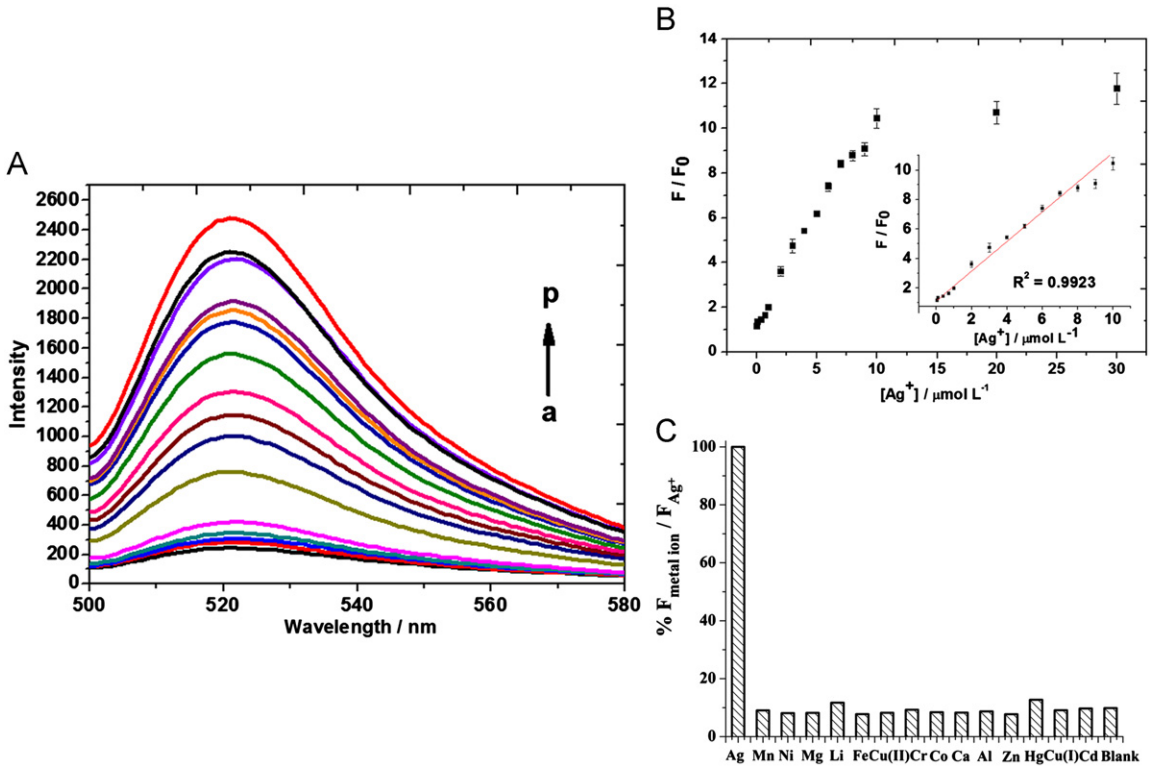

Fig. 5. (A) Fluorescence spectra of FAM-ssDNA upon incubation with a series of different concentrations of Ag^+ ions and 80 μg mL^{-1} GO, from *a* to *p*: 0.05, 0.1, 0.4, 0.7, 1, 2, 3, 4, 5, 6, 7, 8, 9, 10, 20 and 30 μM. (B) Calibration curve for Ag^+ ions detection. (C) Selectivity of the analysis of Ag^+ ions by the method depicted in Fig. 1. The concentration of Ag^+ ions and other competing metal ions were 10 μM.

Table 1
Recovery experiments of Ag^+ ions in East lake water samples.

East lake water	Ag^+ ions added (μM)	Ag^+ ions found (μM)	Recovery (%)
1	0.5	0.46 ± 0.06	92
2	2	2.12 ± 0.23	106
3	5	5.05 ± 0.31	101

proteins through disulfide bonds. The mechanism of this sensing platform was also closely related to the thiol groups. As a strong binder of Ag^+ ions, Cys could interact with Ag^+ ions and removed Ag^+ ions from FAM-ssDNA. Thus, if Cys was introduced to the system, the stronger binding affinity of Ag^+ ions and Cys would result in the release of FAM-ssDNA and the reformation of ssDNA/GO complexes, then a decrease in the fluorescence of the sensing system was detected. Therefore the fluorescence intensity of ssDNA/GO/Ag^+ system was sensitive to Cys and decreased as the concentration of Cys increased (Fig. 6(A)).

To test this idea, the effects of Cys on the fluorescence of the sensing system were investigated. First, 10 μM of Ag^+ ions were introduced to disrupt ssDNA/GO complexes, then various concentrations of Cys were introduced and the fluorescence was monitored. As shown in Fig. 6(B), the fluorescence decreased along with the concentration of Cys increased. A linear relationship ($R^2 = 0.9872$) was observed with Cys from 0.5 to 6 μM and the detection limit for Cys was 0.1 μM (based on a signal-to-noise ratio of 3).

To determine the selectivity of the Cys-sensing system, we studied the effects of SH-containing compounds, such as cystine and glutathione, which always coexisted with cysteine. As shown in Fig. 6(C), neither cystine nor glutathione had the similar fluorescence responses to that of Cys. Furthermore, the effects of the other 19 commonly used amino acids were also investigated. It was clear that only Cys could significantly decrease the fluorescence intensity, and this result suggested that the binding affinity of Ag^+ ions to guanine bases appeared to be much stronger than that to all tested amino acids except for Cys. These results clearly demonstrated that the sensing system was highly selective toward Cys over other amino acids.

Furthermore, we investigated the practicality of this present assay for the analysis of Cys in complex biological samples, such as human urine [35]. The urine samples were obtained from healthy volunteers. Every 1 mL of fresh sample was taken and diluted to 100 mL with water prior to the detection. In these particular urine samples, the endogenous concentrations range from 45 to 170 μM. These are within the normal range reported [36]. A standard addition method was carried out by spiking a certain amount of the Cys standard solution to urine samples, the fluorescence was recorded through the same strategy as depicted above and the fluorescence decreased apparently after urine samples were spiked by standard solutions containing different concentrations of Cys, as shown in Table 2, the corresponding results obtained in human urine samples showed good recovery values, which confirmed that the proposed sensor was applicable for practical Cys detection in real samples with other potentially competing species coexisting.

3.5. Construction of a DNA INHIBIT logic gate

Therefore, a DNA logic gate could be developed using Ag^+ ions and Cys as the two inputs, and the intensity of the fluorescence emission at wavelength 520 nm as the output signal. For input, we defined the presence of Ag^+ ions and Cys as one, and the absence as zero. For output, the normal fluorescence of FAM-ssDNA was considered as one, and quenched fluorescence was defined as zero. With no input or with Cys input alone, the ssDNA/GO complexes showed inherently low fluorescence signal with an

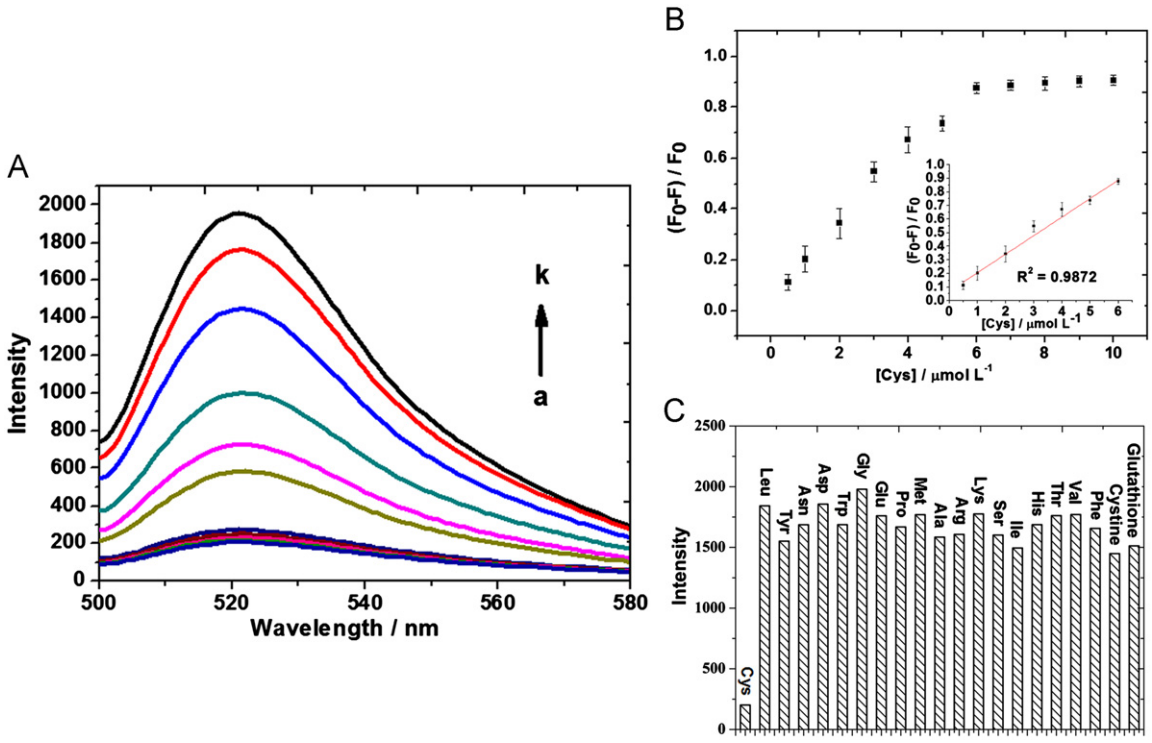

Fig. 6. (A) Fluorescence spectra of FAM-ssDNA upon incubation with 10 μM Ag^+ ions, a series of different concentrations of Cys and 80 μg mL^{-1} GO, from *a* to *k*: 10, 9, 8, 7, 6, 5, 4, 3, 2, 1 and 0.5 μM. (B) Calibration curve for Cys detection. (C) Selectivity of the analysis of Cys by the method depicted in Fig. 1. The concentration of Cys and other inspected species were 10 μM.

Table 2
Recovery experiments of Cys in human urine samples.

Human urine	Cys added (μM)	Cys found (μM)	Recovery (%)
1	0.5	0.48 ± 0.05	96
2	2	2.14 ± 0.18	107
3	5	5.09 ± 0.29	101.8

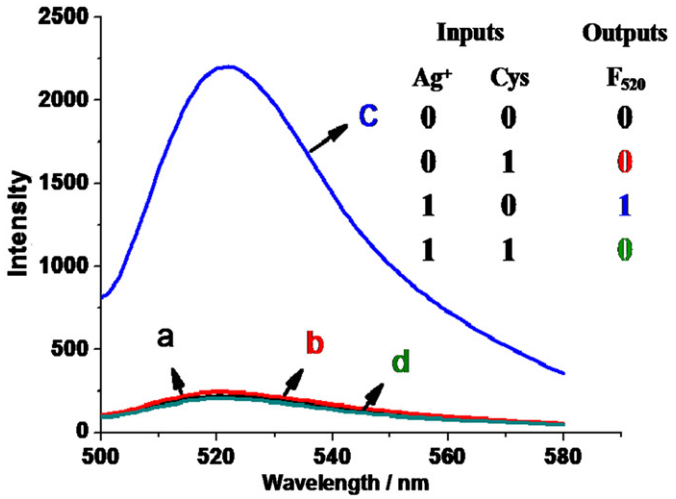

Fig. 7. Operation of the INHIBIT logic gate. Fluorescence spectra of the treatment with Ag^+ ions and Cys after the addition of 80 μg mL^{-1} GO and 0.2 μM FAM-ssDNA: (a) no input; (b) 10 μM Cys; (c) 10 μM Ag^+ ions; (d) 10 μM Ag^+ ions and 10 μM Cys. The inset showed the truth table for the INHIBIT logic gate.

output of zero. With Ag^+ ions input alone, they greatly disrupted the adsorption of FAM-ssDNA on the surface of GO, due to the chelation actions between Ag^+ ions and guanine bases, thus yielded enhanced fluorescence signal, and the output signal of the gate was one. When the system was subjected to the two inputs together, the interaction between Ag^+ ions and Cys released the Ag^+ ions from FAM-ssDNA, resulting in the reformation of ssDNA/GO complexes, causing a decrease in the fluorescence signal, and yielding an output signal of zero. A graph of the output signals of the system was shown in Fig. 7, and the inset was the truth table. Compared with previously published DNA logic gates, the gate operation described here showed excellent digital behavior. The fluorescence of ssDNA/GO complexes could be recovered by addition of Ag^+ ions, while fluorescence in the presence of input Cys alone or both inputs Ag^+ ions and Cys was nearly the same as the initial intensity with no inputs.

4. Conclusion

In summary, we have developed a simple mix-and-detect fluorescence sensor for Ag^+ ions and Cys by using a dye-labeled silver-specific oligonucleotide. This assay is based on the interaction between the target-induced release of the FAM-ssDNA probe and graphene oxide quenching effects, providing several potential advantages: (1) For the first time, we found that Ag^+ ions had a positive effect on the fluorescence intensity of FAM-ssDNA, furthermore, the more deoxyguanosine (G) units the sequence contained, the stronger enhancement that was achieved; (2) The toxicity of heavy metal ions maybe due to the strong interaction between metal ions and nucleobases, the study helps us to understand the influence of heavy metal ions on human health; (3) The DNA strand needs only one dye labeled, leading to less laborious and more cost-effective synthesis; (4) It could not only function with good sensitivity but also exhibit significant "turn-on" fluorescence responses to the metal ions; (5) The planar structure of GO allows it to adsorb multiple kinds of DNA probes. Thus by rational design of the fluorophore and probe sequences,

this simple mix-and-detect strategy could be developed as a multicolor assay for simultaneous detection of multiple targets; (6) Due to the steric-hindrance effects, GO can protect biomolecules from enzymatic digestion or degradation in biological environments. Therefore, we expect that this strategy could be a generalized platform for DNA-based sensing.

Acknowledgment

We gratefully acknowledge the financial support from National Natural Science Foundation of China (Nos. 20805034, 30772058, 20927003, 90913013), Research Fund for the Doctoral Program of Higher Education of China and the National Key Laboratory of Chemo/Biosensing and Chemometrics of Hunan University.

References

[1] S. Shahrokhian, Anal. Chem. 73 (2001) 5972.
[2] S. Seshadri, A. Beiser, J. Selhub, P.F. Jacques, I.H. Rosenberg, R.B. D'Agostino, P.W. Wilson, P.A. Wolf, N. Engl. J. Med. 346 (2002) 476.
[3] M.G. Baron, R.T. Herrin, D.E. Armstrong, Analyst 125 (2000) 123.
[4] J.L. Manzoori, H. Abdolmohammad-Zadeh, M. Amjadi, J. Hazard. Mater. 144 (2007) 458.
[5] J.C. Achenbach, R. Nutiu, Y.F. Li, Anal. Chim. Acta 534 (2005) 41.
[6] A. Mohadesi, M.A. Taher, Talanta 71 (2007) 615.
[7] R.K. Shervedani, M.K. Babadi, Talanta 69 (2006) 741.
[8] R.P. Singh, E.R. Pambid, Analyst 115 (1990) 301.
[9] R.K. Katarina, M.T. Takayana, S. Motomizu, Anal. Chim. Acta 558 (2006) 246.
[10] A. Ceresa, A. Radu, S. Peper, E. Bakker, E. Pretsch, Anal. Chem. 74 (2002) 4027.
[11] K. Kimura, S. Yajima, K. Tatsumi, M. Yokoyama, M. Oue, Anal. Chem. 72 (2000) 5290.
[12] H. Xu, X. Zhu, H. Ye, L. Yu, X. Liu, G. Chen, Chem. Commun. 47 (2011) 12158.
[13] C. Zhao, K. Qu, Y. Song, C. Xu, J. Ren, X. Qu, Chem. Eur. J. 16 (2010) 8147.
[14] W.Y. Xie, W.T. Huang, N.B. Li, H.Q. Luo, Chem. Commun. 48 (2012) 82.
[15] Y. Wen, F. Xing, S. He, S. Song, L. Wang, Y. Long, D. Li, C. Fan, Chem. Commun. 46 (2010) 2596.
[16] J.H. Guo, D.M. Kong, H.X. Shen, Biosens. Bioelectron. 26 (2010) 327.
[17] X.H. Zhou, D.M. Kong, H.X. Shen, Anal. Chem. 82 (2010) 789.
[18] Y.S. Kim, J. Jurng, Analyst 136 (2011) 3720.
[19] B. Li, Y. Du, S. Dong, Anal. Chim. Acta 644 (2009) 78.
[20] D. Liu, Z. Wang, X. Jiang, Nanoscale 3 (2011) 1421.
[21] J. Zhang, L. Wang, H. Zhang, F. Boey, S. Song, C. Fan, Small 6 (2010) 201.
[22] Z. Guo, J. Ren, J. Wang, E. Wang, Talanta 85 (2011) 2517.
[23] R. Yang, J. Jin, Y. Chen, N. Shao, H. Kang, Z. Xiao, Z. Tang, Y. Wu, Z. Zhu, W. Tan, J. Am. Chem. Soc. 130 (2008) 8351.
[24] R. Yang, Z. Tang, J. Yan, H. Kang, Y. Kim, Z. Zhu, W. Tan, Anal. Chem. 80 (2008) 7408.
[25] L. Zhang, T. Li, B. Li, J. Li, E. Wang, Chem. Commun. 46 (2010) 1476.
[26] Z. Chen, X. Zhang, R. Yang, Z. Zhu, Y. Chen, W. Tan, Nanoscale 3 (2011) 1949.
[27] Y. Liu, Y. Wang, J. Jin, H. Wang, R. Yang, W. Tan, Chem. Commun. (2009) 665.
[28] L.B. Zhang, H. Wei, J. Li, T. Li, D. Li, Y.H. Li, E.K. Wang, Biosens. Bioelectron. 25 (2010) 1897.
[29] Z. Zhu, Z. Tang, J.A. Phillips, R. Yang, H. Wang, W. Tan, J. Am. Chem. Soc. 130 (2008) 10856.
[30] S. He, B. Song, D. Li, C. Zhu, W. Qi, Y. Wen, L. Wang, S. Song, C. Fan, Adv. Funct. Mater. 20 (2010) 453.
[31] L. Wang, K.Y. Pu, J. Li, X. Qi, H. Li, H. Zhang, C. Fan, B. Liu, Adv. Mater. 23 (2011) 4386.
[32] W.Y. Xie, W.T. Huang, N.B. Li, H.Q. Luo, Analyst 136 (2011) 4130.
[33] P. Siejak, D. Frackowiak, J. Phys. Chem. B 109 (2005) 14382.
[34] A. Cook, A. Le, J. Phys. Chem. Lab. 10 (2006) 44.
[35] Y.H. Bai, J.J. Xu, H.Y. Chen, Biosens. Bioelectron. 24 (2009) 2985.
[36] E. Kaniowska, G. Chwatko, R. Glowacki, P. Kubalczyk, E. Bald, J. Chromatogr. A 798 (1998) 27.